LAND COVER CLASSIFICATION WITH THE MEDIUM RESOLUTION IMAGING SPECTROMETER (MERIS)

Jan Clevers, Harm Bartholomeus, Sander Mücher and Allard de Wit

Centre for Geo-Information (CGI), Wageningen University and Research Centre, P.O. Box 47, 6700 AA Wageningen, The Netherlands; jan.clevers(at)wur.nl

ABSTRACT

The Medium Resolution Imaging Spectrometer (MERIS) is a payload component of Envisat-1. MERIS is operated over land with a standard 15 band setting acquiring images in the VIS and NIR part of the electromagnetic spectrum. Data are acquired at 300 m (full resolution) and 1,200 m (reduced resolution) spatial resolution over land, thus vegetation can be monitored at regional to global scales. The major merit of MERIS for land applications lies in the provision of (calibrated) data with a spatial resolution intermediate to that of NOAA-AVHRR or SPOT-VEGETATION and Landsat-TM or SPOT-HRV.

This paper describes the results of a preliminary study towards the use of MERIS for land cover mapping in the Netherlands. Full resolution level 1b data of June 16th, 2003, were used in this study. The Dutch land use data base LGN was used as a reference by aggregating the data base from 25 m to 300 m. First, quality and information content of the used MERIS images were explored. Subsequently, the feasibility of the data for land cover classifications was studied. Results showed that MERIS provided only moderate classification results when classifying the major land cover types in the Netherlands using just one image (overall classification accuracy of 49.7 % for seven classes and a Kappa coefficient of 0.369). Partial cloud cover had a negative effect on the accuracies obtained.

Keywords: MERIS, land cover, classification, imaging spectroscopy

INTRODUCTION

A priority research item in Europe (see GMES programme) is mapping and monitoring of land use and land cover (LUC). Actual and reliable information on LUC is needed both for agricultural and environmental applications. The European environment is continuously undergoing change caused by a combination of socio-economic and climatic processes. To protect the environment and to ensure sustainable use of natural resources, a wide variety of national and international legal mechanisms have been established, which on their turn have resulted in various environmental monitoring activities. Examples are the Amsterdam Treaty from 1997, the EU Habitats Directive, the EU Common Agricultural Policy and the Kyoto Protocol.

Remote sensing is the appropriate tool for monitoring large areas such as Europe. Previous approaches were based on the visual interpretation of Landsat-TM and SPOT-XS hard copies at a landscape level in the CORINE land cover project, producing an ecological legend (1). Another approach is (automatic pixel wise) digital classification of the same kind of images into national agricultural land cover maps (2,3,4). However, both approaches use images of high spatial resolution, making this approach expensive and very time-consuming for application at the European scale. At this moment an update of the CORINE land cover data base is being made in the CLC 2000 project.

Other approaches are based on the use of coarse spatial resolution data of, for instance, the NOAA-AVHRR sensor. An example is the pan-European PELCOM land cover data base (5). It used ancillary data on water bodies and urban areas and its overall accuracy at a continental scale is around 60-70 %. For the Netherlands PELCOM includes as classes: grassland, arable land, deciduous forest, coniferous forest, built-up areas and water. Moreover, the coarse scale AVHRR imagery is limiting the use for monitoring purposes due to the fine scale at which most land cover

changes take place in Europe. Various case studies showed that medium resolution images (like those from MERIS and MODIS) can bridge the gap between Landsat/SPOT and NOAA (6,7). Because the area of, e.g., a MERIS pixel is more than ten times smaller than an AVHRR (LAC) pixel, it is expected that a significantly larger number of details can be identified than by using AVHRR-like data. In addition, the high spectral resolution of MERIS is another important feature, which may be exploited to identify more thematic classes (8).

MERIS (Medium Resolution Imaging Spectrometer) is one of the payload components of ESA's Envisat-1, which was launched in March 2002. MERIS is a 15-band, programmable imaging spectrometer, which allows for changes in band position and bandwidths throughout its lifetime. It is designed to acquire data at variable bandwidth of 1.25 to 30 nm over the spectral range of 390-1,040 nm (9). Data will be acquired at 300 m or 1,200 m spatial resolution over land, thus vegetation can be monitored at regional to global scales. MERIS will mostly be operated with a standard band setting. However, it has the capability of in-flight selection of bands for specific applications or experiments. Operational constraints, however, will limit the number and frequency of band changes.

The MERIS spatial resolution of 300 m should be sufficient to monitor heterogeneous terrestrial surfaces at scales required for continental and global change studies (10,11). The objective of this paper was to perform a preliminary study towards the feasibility of using MERIS for land cover mapping at the national scale.

MATERIAL AND METHODS

MERIS data

A full resolution MERIS level 1b data set for the Netherlands was obtained. The data comprised geocoded top of atmosphere (TOA) radiances [W sr^{-1} m^{-2} μm^{-1}] recorded on June 16th, 2003, at about 10:10 UTC. Specifications of the spectral bands are given in Table 1.

Table 1: The 15 spectral bands of the MERIS image of June 16th, 2003.

Band number	Band centre /nm	Bandwidth /nm
1	412.5	9.9
2	442.4	10.0
3	489.7	10.0
4	509.7	10.0
5	559.6	10.0
6	619.6	10.0
7	664.6	10.0
8	680.9	7.5
9	708.4	10.0
10	753.5	7.5
11	761.6	3.7
12	778.5	15.0
13	864.8	20.0
14	884.8	10.0
15	899.8	10.0

Data were converted to ERDAS-IMAGINE format using IDL-ENVI. First, the geocoded data were converted to the Dutch national coordinate system (RD) using the lat/long coordinates of the tie-points and a cubic convolution resampling procedure. The geometric accuracy of the resulting image was within one pixel. Subsequently, a mask was applied in order to create a data set only cov-

ering the Netherlands. Finally, the TOA radiances were converted to TOA reflectances (planetary reflectances) by using the information on TOA solar irradiance [W m^{-2} μm^{-1}] and solar angle ϑ_S according to Eq. 1. The resulting image is depicted in Figure 1. As can be seen, the northern part of the country is covered with clouds. Unfortunately, the cloud flag did not indicate all the clouded pixels and was not used in this study.

$$TOA\ reflectance = \frac{\pi \cdot (TOA\ radiance)}{(Solar\ Irradiance) \cdot \cos \vartheta_S} \quad (1)$$

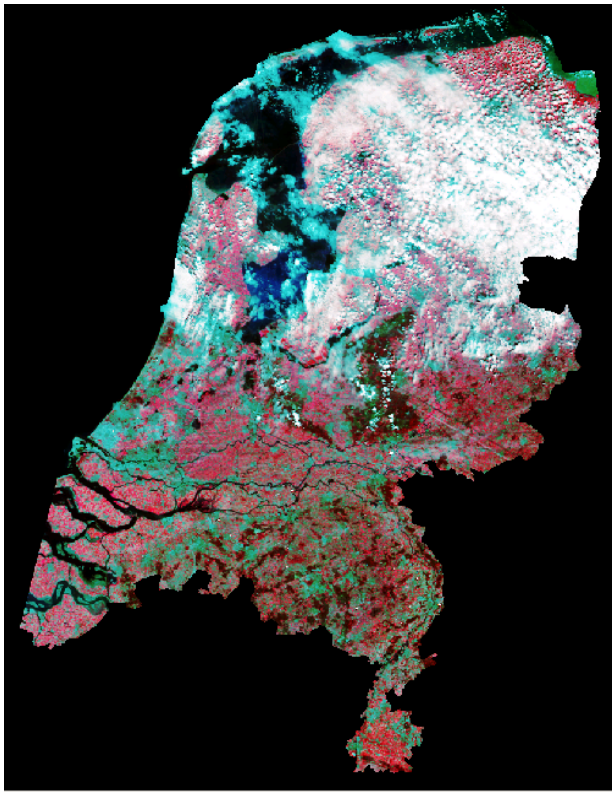

Figure 1: MERIS full resolution image of June 16th, 2003, for the Netherlands. Bands 14, 7 and 5 are depicted in RGB.

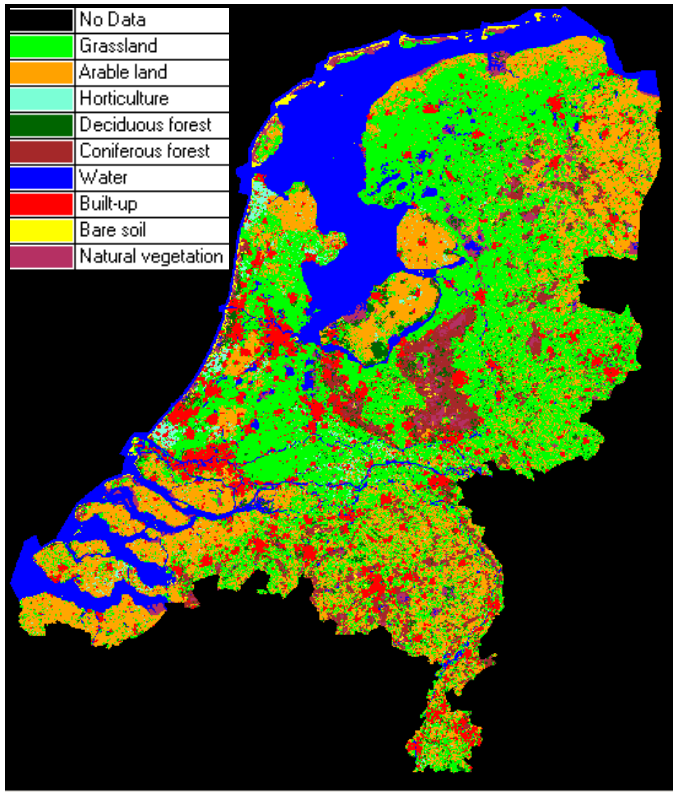

Figure 2: The Dutch land use data base aggregated to 9 classes and 300 m pixel size.

LGN database

The Dutch land use data base (LGN) is a geographical data base that describes the land use in the Netherlands. The data base uses a grid structure with a cell size of 25 metres; the application scale is about 1:50.000. The nomenclature of the LGN4 database contains 39 classes covering urban areas, water, forest, various agricultural crops and artificial, semi-natural and natural land cover classes. LGN is based on multitemporal classification of satellite imagery and integration with ancillary data. Currently, four versions exist (LGN1 - LGN4), which span a time period from 1986 to 2000. For this study the latest version (LGN4), based on satellite data of 1999 and 2000, was used. The original 39 classes were recoded into nine main land cover classes as found in the Netherlands and including those of the previously mentioned PELCOM data base. Subsequently, the grid was aggregated to 300 metres assigning the most frequently occurring class as label. The resulting image is shown in Figure 2. Table 2 shows the frequency distribution of the nine classes. Bare soil relates mainly to areas with sand dunes and covers a relatively small area. Horticulture also covers only a small area. In the analysis presented in this paper the bare soil was added to the natural vegetation and the horticulture was added to the grassland, yielding seven main land cover classes at the end.

Image analysis

In order to study the information content of the MERIS image of Figure 1, a principal component analysis was performed on a subset of the southern part of the Netherlands. In addition, the correlation coefficients between the 15 MERIS bands were mutually calculated. Subsequently, training samples for the main land cover classes were collected using the aggregated Dutch land cover data base as a reference. Per class two polygons of about 50 pixels each were identified in rather homogeneous areas. Thereafter the spectral signatures were studied. Finally, a minimum-distance-to-means supervised classification was performed including clouds as a separate class in the training stage. In a post-processing step, the two subclasses per main cover class were merged. The classification accuracy was evaluated based on a confusion matrix using the whole aggregated land cover data base as a reference (and excluding the class “clouds”).

Table 2: Main land cover types in the Netherlands (derived from LGN4).

Land cover	% of total area
Grassland	36.2
Arable land	23.1
Horticulture	1.3
Deciduous forest	3.0
Coniferous forest	4.6
Natural vegetation	3.1
Bare soil	0.6
Built-up areas	9.9
Water	18.2

RESULTS AND DISCUSSION

Image characteristics

The principal component analysis showed that more than 99% of all information was captured in the first three components (Table 3). The first principal component had particularly high positive loadings for the bands 10 till 15, meaning the bands in the near-infrared (NIR) region, whereas the loadings of the other bands were small. Component 2 had high loadings for bands 1 till 9, representing the visible region, whereas the loadings of the other bands were small. Component 3 mainly exhibited the contrast between bands 7 till 9 and bands 1 till 4, meaning the contrast between bands in the red-edge region as opposed to the blue bands.

Table 3: Results of a principal component analysis on a subset of the MERIS image of June 16th, 2003.

Principal component	1	2	3	4	5	6	7	8	9	10	11	12	13	14	15
Explained variance /%	86.03	12.64	0.59	0.38	0.18	0.09	0.04	0.02	0.02	0.01	0.00	0.00	0.00	0.00	0.00

Table 4 shows the correlation coefficients between the individual spectral bands of MERIS over land. First of all, it can be observed that band 1 and 2 (in the blue) were strongly correlated. Also bands 3 till 8 (all in the visible) were strongly correlated. The latter were also strongly correlated with the former. Subsequently, Table 4 shows that bands 10 till 15 (in the NIR) were strongly correlated. Band 9 at the red-edge slope (at about 708 nm) showed a deviating behaviour, as it was moderately correlated with the visible bands as well as with the NIR bands. It took an intermediate position, making it a particularly interesting band of the MERIS sensor.

In this study the above results were not used for doing a band-reduction before performing, e.g., a classification, but all 15 bands were used.

Table 4: Correlation matrix for a subset of the MERIS image of June 16th, 2003.

r	1	2	3	4	5	6	7	8	9	10	11	12	13	14	15
1	1														
2	.990	1													
3	.961	.990	1												
4	.944	.979	.996	1											
5	.860	.906	.938	.961	1										
6	.852	.907	.948	.969	.975	1									
7	.835	.891	.934	.954	.945	.993	1								
8	.831	.887	.932	.951	.941	.991	.999	1							
9	.632	.688	.735	.780	.914	.861	.824	.821	1						
10	-.011	.002	.010	.046	.261	.085	.009	.004	.515	1					
11	.054	.078	.096	.121	.302	.128	.043	.040	.497	.944	1				
12	-.069	-.061	-.057	-.019	.199	.025	-.047	-.052	.465	.994	.914	1			
13	-.087	-.079	-.075	-.034	.179	.007	-.064	-.068	.458	.990	.912	.997	1		
14	-.066	-.057	-.052	-.016	.198	.025	-.049	-.053	.471	.992	.930	.993	.998	1	
15	-.126	-.108	-.093	-.057	.157	-.013	-.087	-.091	.437	.980	.946	.977	.984	.989	1

Spectral signatures

Figure 3 shows the spectral signatures of the main land cover classes as derived from the MERIS image of June 16th, 2003. The general pattern of the TOA reflectance was as expected. The first few bands showed a relatively high reflectance due to atmospheric scattering. In the NIR the spectral signature showed a dip at about 762 nm (band 11) due to absorption by oxygen in the atmosphere. The spectral signatures of grassland and arable land were very similar, as were the signatures of coniferous forest, natural vegetation and built-up areas. So, these will be most difficult to distinguish.

Classification

Finally, Figure 4 shows the results of a minimum-distance-to-means (MDM) classification for the Netherlands, including also a class “clouds” in the training set. Classification accuracies were determined by using the whole land cover data base (Figure 2) as a reference. Table 5 shows the results for the main land cover classes (without classes bare soil and horticulture as indicated before). Results show a moderate overall classification accuracy of 49.7%. In addition, the Kappa coefficient was calculated as a measure for the agreement between the classified and reference data corrected for chance agreement (12).

Main confusion occurred between grassland and arable land, which was to be expected in the middle of the growing season (similar biomass). Their spectral signatures in Figure 3 already indicated this. Deciduous forest was also confused a lot with grassland and arable land. Coniferous forest was mainly confused with deciduous forest. Built-up areas were particularly confused with natural vegetation, coniferous forest and arable land. This confusion can be explained by the similarity of the spectral signatures of built-up areas, bare soil (as part of the natural vegetation and also occurring in the arable land class) and coniferous forest (often being sparsely vegetated). Water was classified well. These results suggested to merge the grassland, arable land and natural

vegetation classes and to merge the two forest classes as a final post-processing step. Table 6 shows the results for the remaining four main classes. The overall classification accuracy increased to 78.1%. Results were promising even when analysing just one date in the middle of the growing season. When comparing the classified image of Figure 4 with the original in Figure 1, one may observe that cloud cover still will have influenced part of the (not as cloud) classified pixels giving rise to classification inaccuracies. In other words, the accuracies obtained will be conservative ones.

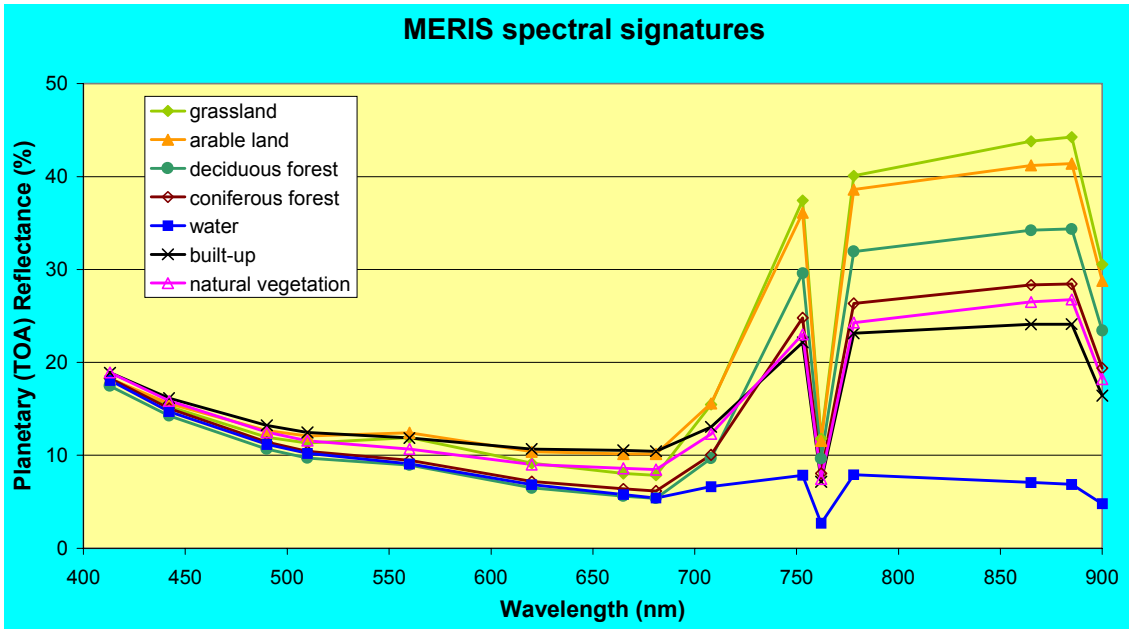

Figure 3: Spectral signatures for the main land cover types derived from the MERIS image of June 16th, 2003.

Table 5: Classification results for the MERIS image of June 16th, 2003.

	Producer's Accuracy	**User's Accuracy**
Grassland	35.2 %	61.2 %
Arable land	62.4 %	36.4 %
Deciduous forest	25.4 %	12.2 %
Coniferous forest	43.3 %	36.4 %
Natural vegetation	16.5 %	8.2 %
Built-up	24.4 %	51.3 %
Water	85.6 %	96.3 %
Overall Accuracy = 49.7 %		Kappa coefficient = 0.369

Table 6: Results of classification into only 4 main classes for the MERIS image of June 16th, 2003.

	Producer's Accuracy	**User's Accuracy**
Agriculture	88.5 %	88.1 %
Forest	56.1 %	28.6 %
Built-up	24.4 %	51.3 %
Water	85.6 %	96.3 %
Overall Accuracy = 78.1 %		Kappa coefficient = 0.622

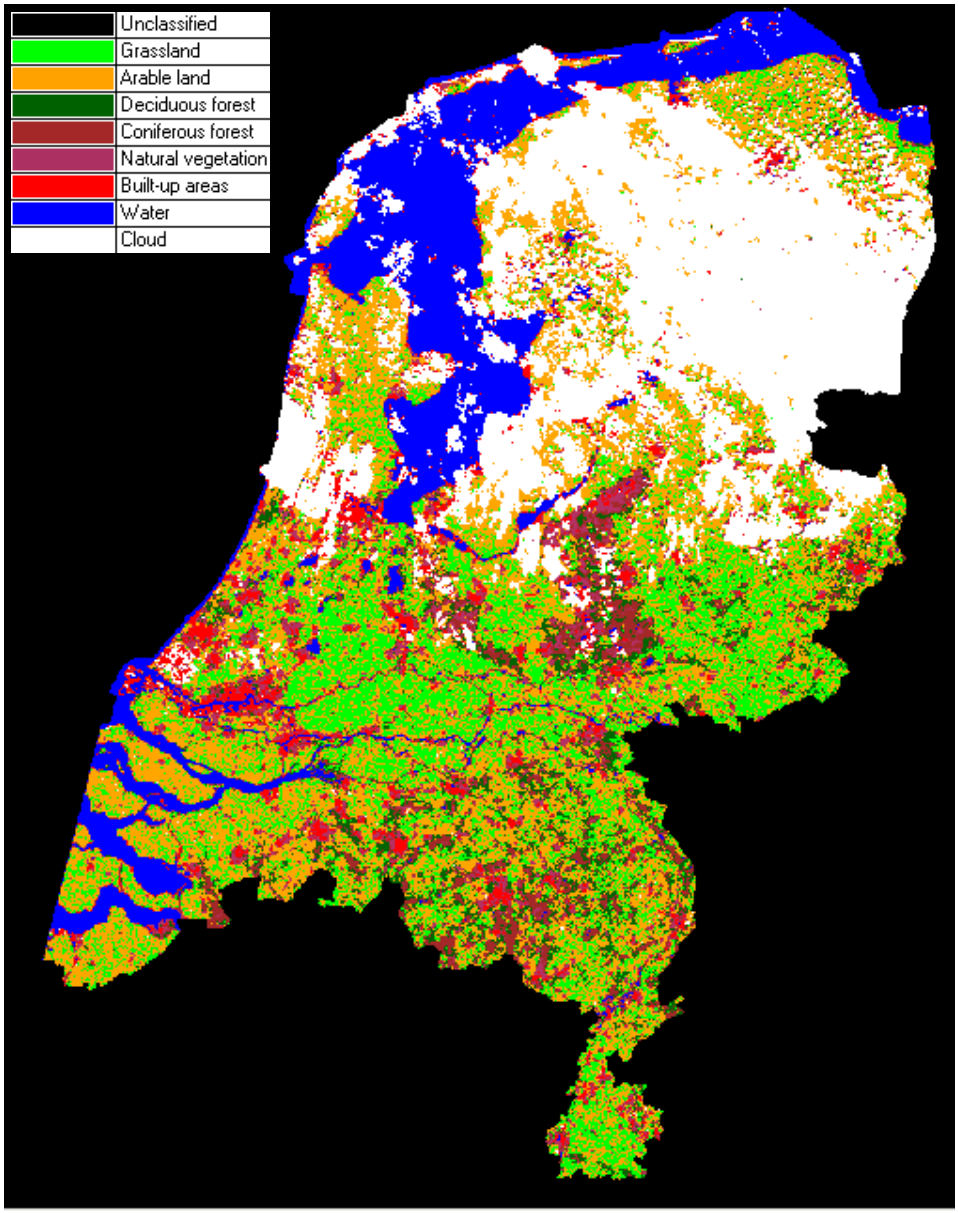

Figure 4: Result of the minimum-distance-to-means classification based on the MERIS image of June 16th, 2003.

CONCLUSIONS

This preliminary study showed that the geometric and radiometric properties of the studied MERIS image of the Netherlands were good. By using the latitude and longitude coordinates that are provided by ESA for a large number of tie points in the image, the national coordinate system of the Netherlands could easily be linked to the image without using additional information. Linking the resulting image to the Dutch land use data base showed that the MERIS image was within one pixel accurate. Using the TOA solar irradiance and the solar angle provided by ESA for the time of image recording as part of the image files one could easily derive spectral signatures in terms of TOA reflectance. The resulting spectral signatures were very suitable for differentiating the major land cover types. The oxygen absorption feature was prominently present at 762 nm, which proved a good spectral positional accuracy of the spectral bands.

Calculation of principal components and correlation coefficients revealed that MERIS provides information over land related to the visible part of the spectrum on the one hand and the NIR part on the other hand. In addition, spectral bands at the red-edge slope of the reflectance curve (in par-

ticular MERIS band 9 at about 708 nm) provided additional information, which may be an important innovative feature of the MERIS sensor for vegetation studies. However, this study does not prove a significant contribution to the multispectral bands over just one VIS and one NIR band for land cover classifications. Future studies should also look at deriving quantitative information from MERIS images, whereby the red-edge position should receive special attention. In this respect, attention should also focus on the use of level 2 MERIS products.

Moderate results were obtained with a monotemporal classification of the land use of the Netherlands. For six classes the overall classification accuracy was 49.7 %, whereas for four classes this increased to 78.1 %. Conservative estimates of the accuracies were obtained, because clouds contaminated some of the pixels used in the accuracy assessment. Further research should focus on multitemporal classifications, extension to other regions in Europe and the use of level 2 MERIS products. Many studies have shown that a multitemporal analysis will provide much better classification results. Therefore, this study really should be considered a preliminary study, and much is expected from a multitemporal analysis of MERIS data.

ACKNOWLEDGEMENTS

This work was performed in the framework of ESA project AO 508. ESA is acknowledged for providing the MERIS data.

REFERENCES

1 EC (1993) CORINE Land Cover: technical guide. Report EUR 12585 (European Commission, Luxembourg)

2 Thunnissen H A M, M N Jaarsma & O F Schouwmans (1992) Land cover inventory in the Netherlands using remote sensing; application in a soil and groundwater vulnerability assessment system. International Journal of Remote Sensing, 13: 1693-1708

3 Thunnissen H A M & E Noordman (1997) National land cover database of The Netherlands: classification methodology and operational implementation. BCRS report 96-20 (BCRS, Delft) 95 pp.

4 Fuller R M, G M Smith, J M Sanderson, R A Hill & A G Thomson (2002) The UK land cover map 2000: construction of a parcel-based vector map from satellite images. The Cartographic Journal, 30(1): 15-25

5 Mücher C A, K Steinnocher, F Kessler & C Huenks (2000) Land cover characterization and change detection for environmental monitoring of pan-Europe. International Journal of Remote Sensing, 21: 1159-1181

6 Addink E A (2001) Change detection with remote sensing; relating NOAA-AVHRR to environmental impact of agriculture in Europe. PhD Thesis (Wageningen University, The Netherlands) 133 pp.

7 De Boer M, J De Vente, C A Mücher, W Nijenhuis & H A M Thunnissen (2000) An approach towards pan-European land cover classification and change detection. NRSP-2 Report 00-18, (BCRS, Delft) 110 pp.

8 Van der Meer F D, J G P W Clevers, S M De Jong, W H Bakker, G F Epema, A K Skidmore & K Scholte (2000) MERILAND: MERIS potential for land applications. USP-2 Report 99-36 (BCRS, Delft) 113 pp.

9 Rast M & J L Bézy (1990) ESA's Medium Resolution Imaging Spectrometer (MERIS): mission, system and applications. SPIE Journal, 1298: 114-126

10 ESA (1995) MERIS: The Medium Resolution Imaging Spectrometer. Report SP-1184 (ESA, Paris)

11 Verstraete M M, B Pinty & P J Curran (1999) MERIS potential for land applications. International Journal of Remote Sensing, 20: 1747-1756

12 Congalton R G & K Green (1999) Assessing the accuracy of remotely sensed data: Principles and practices (Boca Raton, FL: Lewis Publishers) 137 pp.